Efficient consolidation model for morphodynamic simulations in Low-SPM environments

Winterwerp, J. C.; Zhou, Zeng; Battista, G.; Van Kessel, T.; Jagers, H. R.A.; Van Maren, D. S.; Van Der Wegen, M.

DOI
10.1061/(ASCE)HY.1943-7900.0001477

Publication date
2018

Document Version
Final published version

Published in
Journal of Hydraulic Engineering

Efficient Consolidation Model for Morphodynamic Simulations in Low-SPM Environments

J. C. Winterwerp[1]; Zeng Zhou[2]; G. Battista[3]; T. Van Kessel[4]; H. R. A. Jagers[5]; D. S. Van Maren[6]; and M. Van Der Wegen[7]

Abstract: This paper presents a new model, using existing consolidation theory, suitable for long-term morphodynamic simulations; we refer to the dynamic equilibrium consolidation (DECON) model. This model is applicable for muddy systems at small suspended particulate matter (SPM) concentrations, where the sedimentation rates are smaller than the consolidation rates and small fractions of sand can be accounted for. Thus, the model assumes quasi-equilibrium of the consolidating bed. It is derived from the full consolidation (Gibson) equation and is implemented in a mixed Lagrangian-Eulerian bed model guaranteeing stable and non-negative solutions, while numeric diffusion remains small. The erosion and deposition of sand and mud is accounted for, whereas internal mixing (e.g., bioturbation) is modeled through diffusion. The parameter settings for the new consolidation model (the hydraulic conductivity, consolidation coefficient, and strength) can be obtained from consolidation experiments in the laboratory. The model reproduces one-dimensional consolidation experiments and the qualitative behavior of erosion and deposition in a tidal flume. The DECON model was also applied to more natural conditions, simulating fine sediment dynamics on a schematized mud flat and in a schematized tidal basin under tide and wave forcing. The computational results of the mudflat simulations compared well with the simulations with the full Gibson equation. For the tidal basin simulations, DECON predicted the expected landward tidal transport of fine sediment during tide-dominated conditions, while the tidal basin withstood erosion during the more energetic wave-dominated periods. Computational times for the morphodynamic simulations of the tidal basin example without waves increased by a factor of 5 when consolidation was included. For the simulations with waves, this increase in computational times was only a factor of 2, as simulations with waves are always expensive. Applying a complete consolidation model would be prohibitive. The DECON model therefore serves as a useful tool to simulate fine-sediment dynamics in complex wave- and tide-dominated conditions, as well as the effects of seasonal variations. **DOI: 10.1061/(ASCE)HY.1943-7900.0001477.**

Author keywords: Consolidation model; Morphodynamics; Low-concentrated environments.

Introduction

Many natural estuaries, tidal lagoons, and coastal regions contain a mixture of sand and fine, cohesive sediment. In response to natural forcing and/or anthropogenic interference, the shape and bathymetry (morphos) of these systems may change over time. These morphodynamic evolutions affect the hydrodynamics in the system, coupling back to these morphodynamic evolutions. State-of-the-art morphodynamic modeling accounts for the effects of sand only. However, in many cases, the amounts of fines or the changes in morphology are so large that the system's morphology is also affected by the erosion and/or deposition of cohesive sediments. Differently from sand, the deposits of fine sediments (mud) consolidate, thinning and gaining strength with time, which affects the deposit's thickness and mechanical features (stability and erodibility). Because of its high water content, the deformations of fresh mud deposits are large, and the original Terzaghi (1943) consolidation equation is not applicable. The consolidation of such soft mud deposits is commonly described by the Gibson equation (Gibson et al. 1967), which accounts for these large deformations and is generally considered the state of the art for engineering applications. We do not present a detailed derivation of the Gibson equation; for further details, see Mitchell (1976), Schiffman et al. (1985), and other works.

In a stand-alone version, Gibson's equation is widely used for studying and simulating the one-dimensional vertical (1DV) consolidation of mud mixtures in settling columns (e.g., Been and Sills 1981; Schiffman et al. 1985; Toorman 1996; Townsend and McVay 1990). Merckelbach and Kranenburg (2004a) assumed

[1]Senior Specialist, Marine and Coastal Management, Deltares, P.O. Box 177, 2600 MH Delft, Netherlands; Professor, Section of Environmental Fluid Mechanics, Dept. of Civil Engineering and Geosciences, Delft Univ. of Technology, P.O. Box 5048, 2600 GA Delft, Netherlands (corresponding author). Email: j.c.winterwerp@tudelft.nl; han.winterwerp@deltares.nl

[2]Associate Professor, Jiangsu Key Laboratory of Coast and Ocean Resources Development and Environment Security, Hohai Univ., Yankai Bldg., Xikang Rd. 1, Nanjing 210098, China. Email: zhouzeng@hhu.edu.cn

[3]Ph.D. Student, Dept. of Civil, Environmental and Geomatic Engineering, Institute of Environmental Engineering, ETH Zurich, Stefano-Franscini Platz 5, 8093 Zurich, Switzerland. Email: giulia.battista@outlook.it

[4]Senior Expert, Marine and Coastal Management, Deltares, P.O. Box 177, 2600 MH Delft, Netherlands. Email: thijs.vankessel@deltares.nl

[5]Technical Coordinator Software Development, Software Group, Deltares, P.O. Box 177, 2600 MH Delft, Netherlands. Email: bert.jagers@deltares.nl

[6]Senior Expert, Marine and Coastal Management, Deltares, P.O. Box 177, 2600 MH Delft, Netherlands. Email: bas.vanmaren@deltares.nl

[7]Senior Expert, Marine and Coastal Management, Deltares, P.O. Box 177, 2600 MH Delft, Netherlands; Associate Professor, Estuarine Dynamics, IHE-Delft, P.O. Box 3015, 2601 DA Delft, Netherlands. Email: m.vanderwegen@un-ihe.org; mick.vanderwegen@deltares.nl

Note. This manuscript was submitted on January 25, 2017; approved on December 19, 2017; published online on June 15, 2018. Discussion period open until November 15, 2018; separate discussions must be submitted for individual papers. This paper is part of the ***Journal of Hydraulic Engineering***, © ASCE, ISSN 0733-9429.

self-similarity of the mechanical properties of the consolidating mud and introduced a fractal approach for the material functions, as a result of which the consolidation equation can be reformulated as an advection-diffusion equation in a Eulerean frame of reference. Toorman (1996) and later Winterwerp and Van Kesteren (2004) combined the consolidation equation with a hindered settling phase, using a heuristic formula for the transition between the hindered settling phase and the first phase of consolidation, governed by the hydraulic conductivity of the soil. An evaluation of the performance of various 1DV models was presented by Bartholomeeusen et al. (2002).

Recently, Zhou et al. (2016) included Gibson's equation in the Delft3D software for simulating morphodynamic developments in estuarine environments. That model was successfully tested against the development of a virtual tidal mudflat in a tide-dominated environment. Although doable for an isolated mudflat, the large vertical resolution required for real-time resolving consolidation makes the use of the Gibson equation in large-scale and long-term morphodynamic simulations computationally expensive and at times prohibitive.

Hence, there is a need for a cheap consolidation model that can be used for long-term morphodynamic simulations. Sanford (2008) was probably the first to derive such a fast consolidation model. In his multiple-layer model, the vertical dry density distribution was described through an empirical exponential function on the basis of a sediment's equilibrium density profile. This distribution alters in response to the erosion of and sedimentation on the bed at a time scale governed by two empirical relaxation coefficients, the first-order swelling and the consolidation rate, respectively. The strength and erodibility of the consolidating/swelling bed are a function of the time-varying dry bed density. Although Sanford's model is computationally cheap, its parameters cannot be easily determined. Therefore, we need a consolidation model that not only is fast but for which the material parameters are obtainable from simple laboratory tests; thus the model should be based on consolidation physics. This has the additional advantage that the model results can be compared with a complete consolidation model (the original Gibson equation).

These requirements can be met when the time scales for consolidation are small in comparison with the morphodynamic time scale. Hence, we presume a quasi-equilibrium for the consolidation processes. In that case, the equilibrium solution of the consolidation equation can be obtained analytically, yielding an algebraic relation that can be implemented in a morphodynamic model. Thus, the DECON model does not resolve the full time-dependent consolidation process, but it computes the bed-level and mechanical properties at user-defined time intervals. This approach limits the model's applicability to systems with relatively low suspended particulate matter (SPM) concentrations, where the consolidation rates are large in comparison with the sedimentation rates. The new model is therefore not applicable to the conditions under which fluid mud formation occurs, that is, when the sedimentation rates exceed the consolidation rates.

We continue on the Eulerian consolidation model developed by Merckelbach and Kranenburg 2004a (see also Winterwerp and Van Kesteren 2004), in which the material parameters are described with a fractal approach, yielding power law relations. The DECON model is implemented in the generic bed model (GBM) developed by Van Kessel et al. (2011, 2012). This GBM has been coupled to the Delft3D software suite, but it can also be operated stand-alone or coupled to any other morphodynamic model. This implies that the DECON model can run stand-alone or as part of the Delft3D software; in the latter case it would be more appropriate to refer to the DECON module rather than the DECON model. However, in this discussion we refer to the DECON model only and discuss the development of this new model using existing consolidation theory.

The GBM contains a mixed Eulerian-Lagrangian discretization of the bed in multiple layers, shown in Fig. 1. This approach was chosen because of numerical considerations, guaranteeing stable and non-negative solutions, whereas numeric diffusion remains small. The uppermost layer of the model represents the fluffy layer, of which the thickness is undefined (see also Mathew and Winterwerp 2017). Below the fluffy layer, we find the active layer (AL), of variable thickness and variable dry density. This Lagrangian active layer may be subdivided into two or more sublayers, a property used in the new DECON model proposed in this paper. Below the (Lagrangian) active layer(s), a number of Eulerian bed layers are defined (the maximum thickness and the dry density of different sediment fractions are user-defined). However, the thickness and sediment composition may vary over time. The sediment composition in the active and bed layers may vary in response to mixing/bioturbation. If a Eulerian layer becomes too thick, it is split, creating a new Eulerian bed layer above that thickening layer. Similarly, bed layers may disappear when depleted through erosion.

The GBM can deal with multiple sediment classes, some of which may be cohesive and some noncohesive (Van Kessel et al. 2011). The sediment composition may vary in time and space. The exchange of sediment between the bed and the overlaying water column is described as follows:

- Sedimentation from and erosion of coarse, noncohesive sediment takes place in/from the (upper) active Lagrangian layer only; and
- Sedimentation with fine sediment (mud) takes place in the fluffy layer only. Erosion of fine sediments takes place from the fluffy layer and possibly also from the upper active Lagrangian layer.

The exchange of fine sediment between the fluffy layer and the active layer controls the amount of fines in these layers. Mixing and burial further control the amount of sediments (fine and coarse) in the active layer and the bed layers. Bed layers may disappear when depleted, and new bed layers may be created from bed layers that become too thick.

The GBM is also used for modeling the behavior of bed forms and the interaction between various coarser sediments, such as the interaction between sand and gravel (e.g., Blom 2003; Sloff et al. 2006).

In the DECON model, we maintain the structure of the GBM with its fluffy, active, and bed layers. This model is described in detail in the next section. The discretization of the model formulations is explained in the Appendix. The model's performance is assessed against a number of simple test cases, including two morphodynamic simulations.

Quasi-Equilibrium Model for Consolidation in Low-SPM Environments

To detail the description of the generic bed model (GBM), the DECON model contains the following features (Fig. 1):

1. The fluffy layer contains mud only, and its thickness is not defined but its mass is. The fluffy layer is subject to consolidation (transport to the upper active layer) but not to strength development. Thus, its erodibility remains constant according to user-defined parameters (see Appendix). The erosion and deposition of mud may take place from/on this layer. Although the dry density in the fluffy layer is not defined, typical values would amount to the gelling concentration (50–150 g/L). Thus,

J. Hydraul. Eng., 2018, 144(8): 04018055

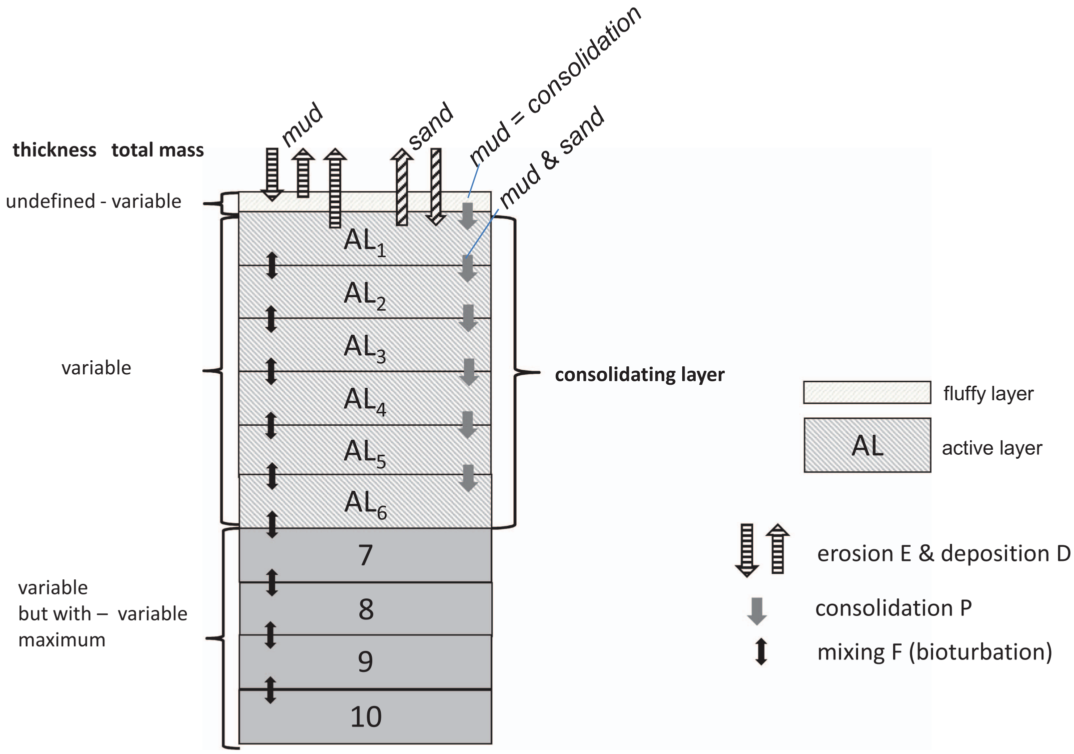

Fig. 1. (Color) Discretization of bed layers in the DECON model, modified from the generic bed model.

our approach remains consistent with other applications of the fluffy-layer concept (Mathew and Winterwerp 2017).

2. The active layers have a variable thickness and variable dry density and may contain sand and mud. The erosion of mud may take place from the upper active layer as well, to account for spatial inhomogeneities (within a computational cell). The erosion and deposition of sand take place only from/on the upper active layer. The mechanical properties (erodibility) of the active layer change with consolidation and mixing.
3. The Eulerian bed layers have varying thickness and mass (dry density).
4. The active layer is split into six sublayers (but the user may choose otherwise). Consolidation takes place in these active sublayers; we refer to the consolidating layers. The user defines when the (equilibrium) mechanical properties of these layers are to be updated. The total thickness of these six consolidating layers is represented by Δ_c, which is a function of time and which is determined by the total mass in the active sublayers; this is the Lagrangian functionality. The relative thickness of the six consolidating sublayers is user-defined, depending on the relevant time scales of the problem at hand.
5. When the total thickness of the consolidating sublayers (the sum of the active layers) exceeds a user-defined value, the sediment is buried from the lowest active layer into the upper bed layer. This buried sediment immediately attains the predefined mechanical properties of that bed layer. Sediment is never advected from the bed layers toward the active layers, except by the process of mixing/bioturbation. New active layers can be formed only from deposition.
6. During erosion, the active layers may be eaten away one by one, depending on their mechanical properties. In that case, the sediments in the active layer are not supplemented from the bed layers below. During erosion, the bed becomes overconsolidated—too strong—given the reduced mass in the eroding bed. Therefore, all the bed processes, consolidation, and mixing (bioturbation) stop. Active layers are reformed or refilled only from sedimentation. When an active layer regains the thickness it had before the erosion event, the consolidation processes become active again. The user is advised to choose the model parameters such that the active layers never disappear completely, to prevent a discontinuous buildup of the bed properties.
7. If all active layers were eaten away by erosion, the first bed layer would be eroded; the erosion parameters of the bed layer are constant and user-defined.
8. Consolidation is governed by the mud fraction only. Sand is passive, only determining the hydraulic conductivity and effective strength of the soil.
9. The bed layers below the six consolidating layers maintain their original properties and functions, which are user-defined, although their mass, thickness, and composition may change over time by burial from the consolidating layers, by erosion when all the consolidating layers have been eroded, and/or by bioturbation (mixing).

Although layers may disappear and be regenerated, from a numerical point of view it is not advisable that this disappearance/regeneration occurs too often. The layers should therefore be thick enough to survive a number of consecutive erosion events. The proposed layer distribution is therefore based on the presumption that the erosion of the bed is governed by four time scales, which are typically

1. the tidal time scale, in which the sediments in the water column are more or less in equilibrium with a thin soft layer of fine sediment on the bed (the fluffy layer); around slack water, this layer is typically a few millimeters to a few centimeters, at most; inclusion of this fluffy-layer concept is crucial for simulating the net sediment transport by tidal asymmetry and other processes;
2. the spring-neap cycle, in which part of the fines in the fluffy layer may gain strength/consolidate, as fines are buried

within the upper active layer, and in this way fines may accumulate on/in the bed during neap tide, to be remobilized during spring tide;

3. the seasonal time scale, in which fines are subject to biological activity [bioturbation, biostabilization (algae), and biodestabilization (benthic fauna)], and storm conditions; and
4. the decadal time scale, in which extreme events such as storms and floods may have a profound effect on the long-term morphodynamics of the system.

Fig. 1 shows a diagram of the generic bed model adapted to the new consolidation formulations. As discussed previously, we presume that consolidation is relatively fast, further to our assumption of low concentrated suspensions under low dynamic conditions. This implies that mechanical equilibrium is obtained fast. The basic idea behind the new consolidation model is that this equilibrium is achieved within a user-defined time scale (consolidation time step T_c), similar to the approach in morphodynamic modeling. Thus, within such a consolidation time step, the mechanical properties of the bed remain constant, as do the erosion properties of the bed.

The new consolidation model is based on the Gibson equation for consolidation in a Eulerian frame of reference. The relevant equations for the consolidation of mud are, assuming a self-similar (fractal) structure of the consolidating bed (see Merckelbach and Kranenburg 2004a or Winterwerp and Van Kesteren 2004 for the derivations)

$$\frac{\partial c_m}{\partial t} - \frac{1}{\rho_s}\frac{\partial}{\partial z}[\Delta_\rho k c_m^2] - \Gamma_c \frac{\partial^2 c_m}{\partial z^2} = 0 \tag{1}$$

$$\begin{aligned}
\Gamma_c &= \frac{2}{3-n_f}\frac{K_k K_p}{g\rho_w} = \text{consolidation coefficient (constant)}\\
k &= K_k(\phi_m/(1-\phi_s))^{-2/(3-n_f)} = \text{hydraulic conductivity}\\
\sigma'_v &= K_p(\phi_m/(1-\phi_s))^{2/(3-n_f)} = \text{effective stress}\\
\phi_m &= \frac{c_m}{\rho_s};\phi_s = \frac{c_s}{\rho_s}
\end{aligned} \tag{2}$$

where subscripts m and s refer to the bulk mud and sand fraction, that is, the sum of all mud and all sand subfractions, respectively, in the computational domain; ϕ and c are volumetric concentration of the solids and the solid's mass concentration; ρ_w and ρ_s are specific density of water and sediment; $\Delta_\rho = (\rho_s - \rho_w)/\rho_w$ = relative density; and t and z are time and the vertical coordinate (positive upward). The material parameters for the effective stress K_p (Pa), hydraulic conductivity K_k (m/s), and sediment structure n_f (fractal dimension) follow from laboratory experiments (e.g., Merckelbach and Kranenburg 2004b) or if unavailable, from the literature (see also the Appendix). These equations are valid for small sand concentrations only, that is, well beyond the criterion for cohesive bed behavior (Winterwerp and Van Kesteren 2004); the sand content should not exceed a few ten percent, as the consolidation equation is no longer valid at higher sand concentrations. As the DECON model is coupled to the Delft3D software, the effects of hindered settling are accounted for in the water (sediment transport) phase.

In the DECON model, we make explicit use of the total mass of sediment in the consolidation layer (the six active sublayers). This total sediment mass determines the Gibson height for the total sand content and total mud content, ζ_s and ζ_m, respectively

$$\zeta_m \equiv \int_{\Delta_c} \frac{c_m}{\rho_s - c_s}\mathrm{d}z \quad \text{and} \quad \zeta_s \equiv \int_{\Delta_c}\frac{c_s}{\rho_s}\mathrm{d}z \tag{3}$$

where c_m and c_s are mass concentration of all the mud and of all the sand fractions, respectively, in the active layers; and Δ_c = total thickness of the consolidating layer. For the equilibrium conditions, $\partial c/\partial t = 0$ (e.g., Merkelbach and Kranenburg 2004a), and Eq. (1) can be integrated over the thickness of the consolidating layers Δ_c

$$\Delta_c(T_c) - \zeta_s - z = \frac{n}{n-1}\frac{K_p}{g(\rho_s - \rho_w)}\left(\frac{c_m}{\rho_s}\right)^{n-1} \quad \text{with } n = \frac{2}{3-n_f} \tag{4}$$

where T_c = consolidation time, which is much larger than the time step in the hydrodynamic and sediment transport model (the driving forces) but much smaller than the relevant time scales in the driving hydrodynamics (e.g., the semidiurnal tide or the spring-neap cycle). Thus, T_c is the time step for updating the equilibrium density distribution and hence the strength distribution relevant for erosion. Of course, T_c should be larger than the physical consolidation time, for which a typical time scale amounts to δ^2/Γ_c, and thus typically of the order of minutes to a few hours at most for suitable DECON applications. Eq. (4) can be integrated over the consolidating bed layer

$$\Delta_c(T_c) = \zeta_s + \frac{n}{n-1}\frac{K_p}{g(\rho_s-\rho_w)}\left(\frac{g(\rho_s-\rho_w)}{K_p}\zeta_m\right)^{\frac{n-1}{n}} \tag{5}$$

in which Δ_c is the thickness of the consolidating layers (the six active layers), and of which the value varies at the time scale T_c. From this relation, we obtain the equilibrium distribution of the mass concentration for the sediment (mud content only), often referred to as the dry density distribution (bulk or total mud content)

$$\frac{\rho_{\text{dry}}(z)}{\rho_s} \equiv \frac{c_m(z)}{\rho_s} = \left[(\Delta_c(T_c) - z - \zeta_s)\frac{n-1}{n}\frac{g(\rho_s-\rho_w)}{K_p}\right]^{\frac{1}{n-1}} \quad \text{for } 0 < z < \Delta_c(T_c) - \zeta_s \tag{6}$$

Although we can model more than one mud class in the water column, these are summed in establishing the consolidation properties of the bed. If sand is present, it is transported by mixing and burial and not through consolidation. However, sand affects the material parameters in the consolidation model [Eq. (2)].

Next, we define the exchange processes with the water column. The exchange processes between the various layers are described in the Appendix. In the DECON model, the total mass of sediment in the bed model may change because of erosion/sedimentation at the computational time steps of the sediment transport model. However, the thickness and sediment properties (erodibility, in particular) are updated only every T_c time steps. This might imply a stepwise change in the erosion properties, inducing irregularities in the SPM distribution. Therefore, we propose introducing a relaxation time in the zero-order erosion parameter M_E (e.g., Winterwerp et al. 2012 for more details on this erosion model)

$$\begin{aligned}
E &= \alpha_E \frac{\Gamma_c \rho_{m,dry}^2}{10\rho_s c_u D_{m,50}}(\tau_b - \tau_{cr})\left(1 - \exp\left\{\frac{m_{\text{rel}}\Delta t}{T_c}\right\}\right)\\
&\equiv \alpha_E M_E(\tau_b - \tau_{cr})R_{rel}
\end{aligned} \tag{7}$$

where the erosion parameter M_E has the dimension kg/m^2 s Pa≡ s/m; Δt = computational time step of the sediment transport model; and m_{rel} = user-defined relaxation coefficient for erosion. For instance, for $m_{rel} = 0.3T_c/\Delta t$, one would attain 95% of the equilibrium erosion rate in 10 computational time steps. The coefficient α_E is a user-defined, spatially varying parameter to account for spatial inhomogeneities (default value = 1). Note that the erosion formula of Eq. (7) was obtained by assuming that the erosion rate is limited by the swelling rate of the soil (e.g., Winterwerp et al. 2012). The undrained shear strength c_u is approximated by the yield strength (e.g., Winterwerp and Van Kesteren 2004), again assuming self-similar behavior (Kranenburg 1994)

$$c_u \approx \tau_y = K_y(\phi_m/(1-\phi_s))^{2/(3-n_f)} \tag{8}$$

where the coefficient for yield strength K_y (Pa) follows from vane tests in the laboratory (user input). The critical shear strength for erosion is related to the plasticity index PI of the sediment mixture

$$\tau_{cr} = \alpha_\tau \gamma_{cr} \mathrm{PI}^\beta \text{ with } \beta = 0.2 \text{ and } \gamma_{cr} = 0.7 \text{ Pa} (0.35 < \gamma_{cr} < 1.4 \text{ Pa})$$
$$\mathrm{PI} = A(X^{cl} - X^{cl}_{cr}) \text{ with PI in } [\%]$$
$$X^{cl} = \alpha_{cl} X^{\text{mud}} \text{ assuming a constant clay-silt ratio,}$$
$$\alpha_{cl} \text{ user-defined input} \tag{9}$$

where PI = plasticity index; A = activity; X = total mud or clay content; and $\alpha_\tau(x, y)$ is a user-defined calibration parameter, which may vary horizontally (x, y) over the computational domain (for example, different in channel and on tidal flat) and has default value = 1. The effect of sand on the erosion of the cohesive bed is accounted for through the PI. Methods to determine values for PI, A and the critical clay content X^{cl}_{cr} can be found in Winterwerp et al. (2012) and Winterwerp and Van Kesteren (2004).

Vertical Discretization of the Consolidation Model

In this section we discuss the vertical discretization of the DECON model. Fig. 2 shows a typical vertical dry density profile for equilibrium conditions. The convex-up power-law profile is very steep near the bed surface. Therefore, we propose the distribution of the active and bed layers in the consolidating layer shown in Fig. 2 and presented in Table 1.

The consolidation time step T_c is input by the user and its value is determined in relation to the relevant time scales of the various morphodynamic processes. However, the vertical density profile is updated only in the case of accretion [$(\mathrm{d}\zeta_m/\mathrm{d}t + \mathrm{d}\zeta_s/\mathrm{d}t) > 0$]. If the bed is in erosive mode, the vertical dry density profile is not updated, allowing the lower, stronger layers to be exposed to erosion. Hence, we have introduced three numerical time scales. The first time scale yields the computational time scale Δt for the water–bed exchange processes (and the sediment-transport model), which also governs the sediment fluxes from and to the bed (e.g., erosion and sedimentation). The second time step is the consolidation time step T_c, that rules the transition of the dry density profile in the consolidating layers to its equilibrium profile, determining the mechanical properties of the bed, including the effects of bioturbation. Finally, a morphodynamic time scale T_m is used but is not further discussed in this paper (e.g., Roelvink 2006).

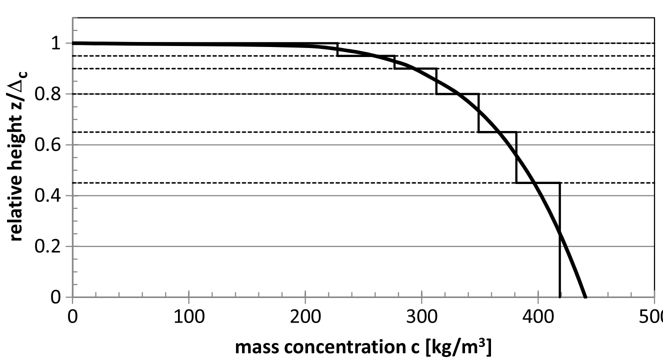

Fig. 2. Example of typical distribution of mass concentration at final consolidation with discretized distribution. The thick line represents an equilibrium density distribution, whereas the thinner staircased line represents the model's discretization.

Table 1. Typical layer distribution in consolidating bed (user input)

Layer number	Relative thickness
Active Layer 1	$\delta_{AL1} = 0.05\Delta_c$
Active Layer 2	$\delta_{AL2} = 0.05\Delta_c$
Active Layer 3	$\delta_{AL3} = 0.10\Delta_c$
Active Layer 4	$\delta_{AL4} = 0.15\Delta_c$
Active Layer 5	$\delta_{AL5} = 0.20\Delta_c$
Active Layer 6	$\delta_{AL6} = 0.45\Delta_c$

Testing the DECON Model

The DECON model is tested against two simple experiments and then applied using an existing case study of a tidal flat and a large-scale numerical morphological experiment. The four experiments, subsequently elaborated, are

1. a consolidation column to obtain the model's consolidation parameters and to test the proper implementation of the equations;
2. a hypothetical tidal flume with erodible bed, assessing the response of the model to tidal variations in the flow velocity and to the sediment supply;
3. a tidal flat to evaluate the consolidation behavior in response to tide-induced sedimentation and a comparison with the full Gibson model by Zhou et al. (2016); and
4. a morphodynamic simulation of a hypothetical, schematized tidal basin that assesses the large-scale behavior of the consolidation model in response to tides and waves.

Consolidation Column

The DECON model was tested against the measured equilibrium heights obtained from laboratory consolidation experiments for muds from the relatively sheltered Dutch Wadden Sea, from the Gulf of Martaban (a fine-grained exposed deposit of the Irrawaddy Delta in Myanmar), and from the Dutch freshwater lake, Lake Markermeer (Fig. 3). Settling experiments in previous studies (not reported here) were analyzed using the consolidation model of Merckelbach and Kranenburg (2004b) to obtain the material parameter settings. The same parameter settings were implemented in DECON and the output of the new consolidation model compared to observations.

The measured and computed interface heights (Fig. 3) shows excellent agreement. This was encouraging, given (1) the wide range in environmental settings (exposed marine settings to sheltered fresh water); and (2) no need for calibration/fine-tuning. Fig. 4 shows the equilibrium vertical dry density profile for an example of Lake Markermeer. This dry density distribution was measured with an acoustic sensor, which is highly sensitive to gas; the large outlier shown in Fig. 4 at $z \approx 0.1$ m is due to a small gas bubble in the soil. The outlier shown at the sample's surface is attributed to the measuring volume of the acoustic sensor. Table 2 presents the material parameters obtained by the method of Merckelbach and

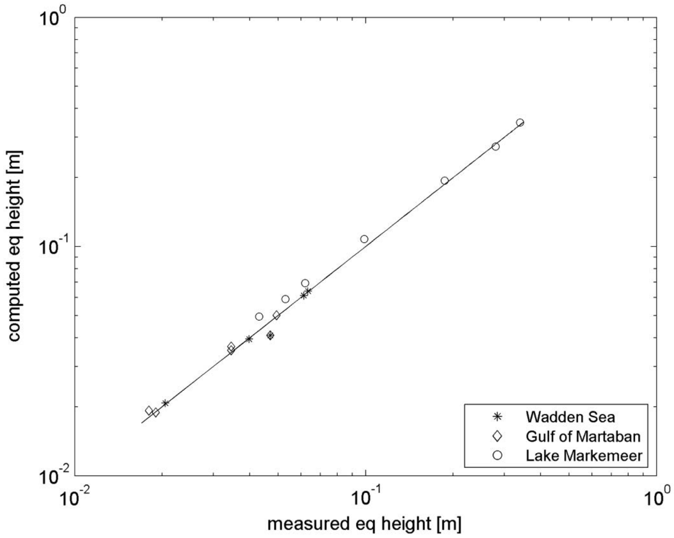

Fig. 3. Comparison of computed and measured equilibrium heights.

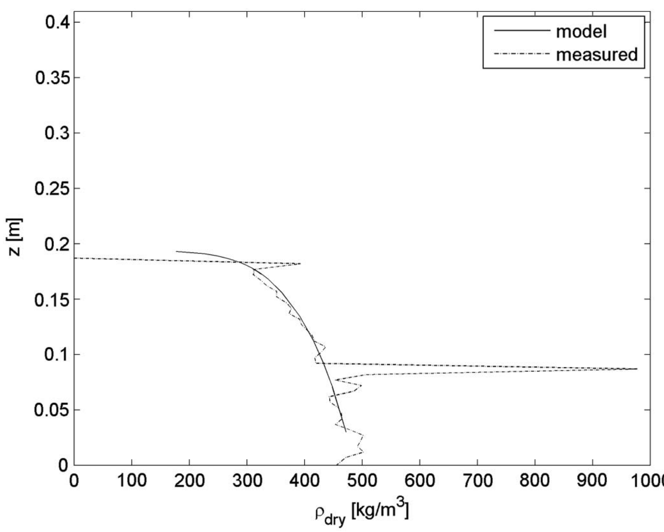

Fig. 4. Comparison of computed and measured density profiles at equilibrium for mud from Lake Markermeer.

Kranenburg (2004b) from analyzing the settling curve of the consolidation experiments (results not shown).

Note that the material parameters for hydraulic conductivity K_k [which follows from the full consolidation model of Winterwerp (1999)] are not required for the equilibrium consolidation model, although they implicitly determines the consolidation coefficient Γ_c. Moreover, K_k does influence the erosion parameter M_{E} (the subject of the second experiment), also through the consolidation coefficient Γ_c.

Sedimentation and Erosion in a Tidal Flume

Next, sedimentation and erosion by tidal flow and the resulting bed level variations in a 5-m-deep and 5-km-long flume were studied to evaluate the response of the bed to variations in flow velocity and sediment supply. The water level at the downstream boundary was kept constant at 2 m, while at the upstream boundary we prescribe a semidiurnal M_2 tide (velocity amplitude 0.4 m/s) and M_4 overtide

Table 2. Material parameters for consolidation experiment shown in Fig. 4 [e.g., Eq. (2)], where h_0 and c_0 are the initial height and sediment concentration of the consolidation experiment

Parameter	Value
h_0 (cm)	40
C_0 (g/L)	200
K_k (m/s)	1.59×10^{-13}
n_f	2.69
K_p (Pa)	1.99×10^{7}
$h_{\infty,obs}$ (cm)	18.7
$h_{\infty,model}$ (cm)	19.4

(velocity amplitude 0.1 m/s at a phase difference relative to M_2 of 45°, resulting in a peak bed shear stress of 0.53 Pa). The inflowing SPM concentration was initially set to 1.0 kg/m^3, resulting in a period of net accretion in the flume, followed by an inflowing SPM concentration of 0.01 kg/m^3 yielding a net erosion of the bed. The initial 1-m-thick sediment bed had a vertically uniform dry density of 265 kg/m^3. The consolidation time step was set at 5 times the hydrodynamic/sediment model time step. This factor of 5 was relatively small and could be enlarged to speed up the simulation. Note that the relatively high SPM boundary condition would violate the applicability of the model, but it was chosen to show the model's response within a reasonable simulation time.

The critical shear stress for erosion was set at 0.225 Pa, which is in the range of values for fine, poorly consolidated sediment. In this model setup, the parameters α_t and α_E were misused to set the model parameters and speed up the model response; they were set to $\alpha_\tau = 0.05$ and $\alpha_E = 0.04$. The settling velocity was set at 1 mm/s (representing flocculated sediments), and the erosion parameters were computed by the model using Eq. (7) with the material properties provided in Table 2 and $D_{50} = 30$ μm. Fig. 5 shows the evolution of the computed bed level and density profile in time (for a period of 6 days) halfway along the flume ($x =$ 2.5 km), with a zoom-in on the upper 12 cm of the bed in Fig. 5(b). During the first three days of the simulation, the bed accreted, although some erosion occurred during accelerating tide, eating away the two upper layers. The deposited sediments were buried in the lower layers by the process of consolidation, and the bed became thicker. After three days, the M_2 and M_4 tide became in phase, increasing the mean stress beyond the critical value, and net erosion of the bed occurred. Layer after layer was eaten away by the erosion. However, around the slack water, some sedimentation still occurred. Note that the fluffy layer is not depicted in these graphs.

Sedimentation on a Tidal Flat

The consolidation model developed by Zhou et al. (2016) (on the basis of the full time-dependent solution of Gibson's consolidation equation) was tested against the development of a virtual tidal mudflat. We used one of their hypothetical cases, a 2,700-m-long cross section with an initial depth of 4 m below mean sea level and a mean tidal range of 5 m, and compared Zhou's model with the DECON model results. Both models were implemented in the same numerical environment, the generic bed model of the Delft3D software, but they differed in several aspects, the most important being that the DECON model computes the consolidation in quasi-equilibrium over a time step much longer than the hydrodynamic time step, whereas Zhou's model solves the Gibson's equation at each hydrodynamic time step. Both models applied the same numerical setting as Zhou et al. (2016), apart from the layer distribution. In DECON, the 20 layers were set at the relative

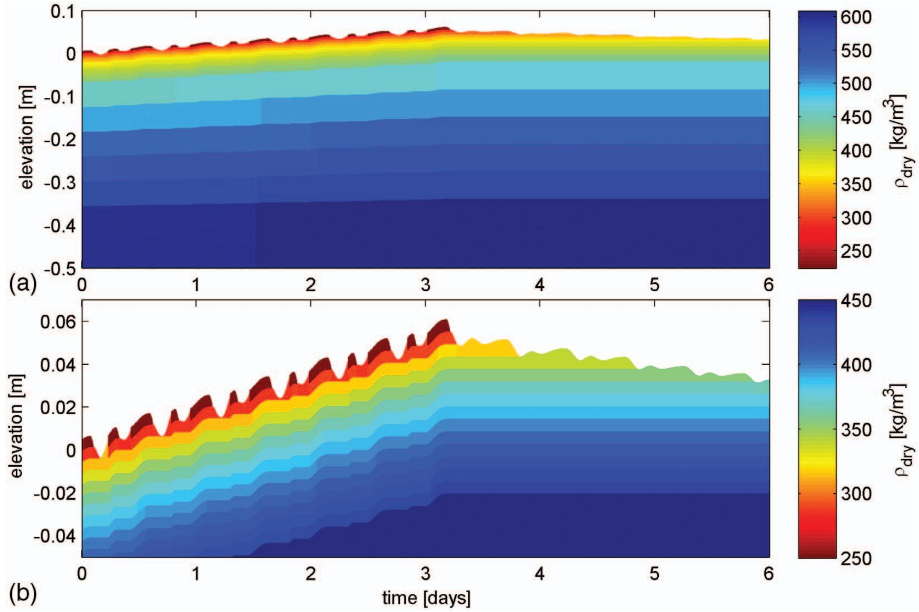

Fig. 5. (Color) Computed bed development at x = 2.5 km with the complete bed profile and details near-surface with active and bed layers. The fluffy layer is not depicted (note different density scales).

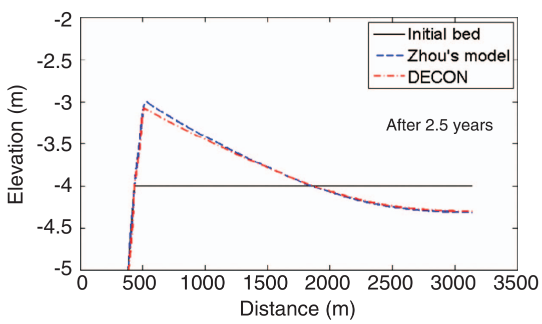

Fig. 6. (Color) Bed level after 2.5 years of simulation, computed with DECON and Zhou's model.

distribution of 0.01, 0.01, 0.015, 0.015, 0.025, 0.025, 0.025, 0.025, 0.025, 0.025, 0.05, 0.05, 0.05, 0.05, 0.075, 0.075, 0.1, 0.1, 0.125, and 0.125, whereas in Zhou's model, the upper layer's thickness was set at a constant value of 2 cm, and the 19 lower layers had a constant thickness of 10 cm. In comparing the model results, we focused primarily on the differences between Zhou's model and the DECON model; for a detailed description of the case and a physical interpretation of the results, see Zhou et al. (2016).

The bed level changes computed with Zhou's model and the DECON model compared well (Fig. 6), although DECON predicted slightly more consolidation. This is also apparent in Fig. 7, which shows the computed density profiles after 2.5 years of morphodynamic simulation. The dry densities computed with DECON were a bit higher than in Zhou's model, which is explained by the following:

1. The DECON density profiles were always at equilibrium, whereas equilibrium in Zhou's model had not yet been attained.
2. Possibly more important were the user-defined conditions in the active layer of Zhou's model. In the current simulations, the user-defined dry density in Zhou's active layer was set at 150 g/L, whereas in DECON, the dry density in the upper layers is determined by the equilibrium model.
3. This difference in active layer conditions affected not only the effective consolidation processes but also the mechanical properties of the active layer, and thus the erosion of the bed at larger velocities.

Despite these differences, we may conclude that for this tidal flat test case, the performance of the DECON model matched that of the full Gibson model, as implemented by Zhou, and the computational time decreased from 9 to 3.5 h on a personal computer (PC) with a Core i7-4810MQ@2.8GHz processor (Intel, Santa Clara, California).

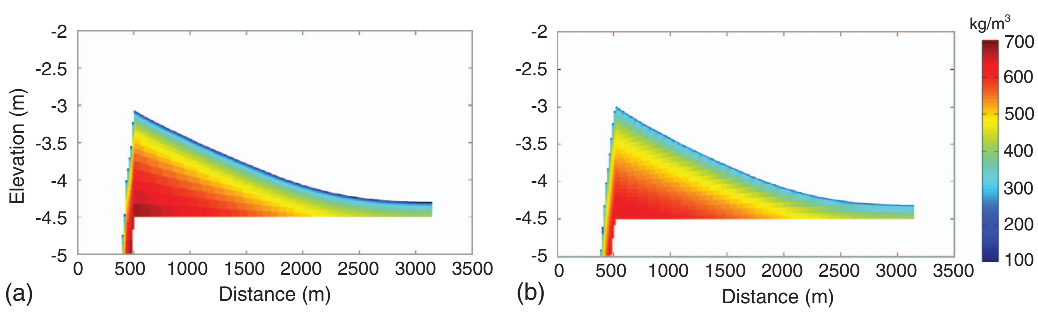

Fig. 7. (Color) Dry density distribution in the bed after 2.5 years of simulation: (a) DECON; and (b) Zhou's model.

Sedimentation and Erosion in a Schematized Tidal Inlet

In a fourth test, we applied the DECON model for simulating the morphodynamic evolution of the intertidal area of a hypothetical, schematized tidal inlet. Essential for the evolution of such intertidal areas is that fine sediments (1) accumulate on tidal flats by settling and scour lags (van Straaten and Kuenen 1957; Postma 1961); and (2) subsequently build up strength to resist erosion during winter storms. The proper modeling of settling and scour lag requires the implementation of a fluffy layer concept (Mathew and Winterwerp 2017), and strength buildup requires the modeling of consolidation. The conventional sediment transport models without consolidation do not account for these processes and therefore fail in simulating the long-term evolution of muddy sediments in tidal inlets. In this section, we show how the DECON model generated credible trends in this long-term evolution.

A tidal inlet typically consists of an outer ebb-tidal delta, a channel intersecting the coastline, and a lagoon with an intricate pattern of tidal channels decreasing in size in landward direction. The hydrodynamic energy in such systems decreases in landward direction as a result of decreasing tidal velocities and sheltering from wave energy. Over longer time scales, fine sediments are transported toward the head of the inlet by tidal currents, forming intertidal mudflats. These sediments consolidate, thereby gaining strength, and may become able to withstand erosion during extreme storm events.

The schematized tidal inlet was created from a Delft3D simulation, starting from an initial flat bed consisting of 0.1-mm-diameter sand. The model was forced by a semidiurnal tide with an amplitude of 3 m for a period of 100 years, using the standard van Rijn (2007a, b) sediment transport formulations. The resulting bathymetry (Fig. 8) was used as the initial bed level for fine sediment simulations using the DECON model. The effect of consolidation is tested by running the Delft3D model for mud only, and comparing computational results with (i.e., DECON) and without consolidation. DECON is run for 25 years. In one series simulations with tide-only are done. In a second series, a 25-year composite forcing was prescribed with each year 10 months of tide-only and then 2 months of tide and waves (storm conditions). These storm conditions were accounted for with SWAN software simulations with a significant wave height and period of $H_s = 1.5$ m

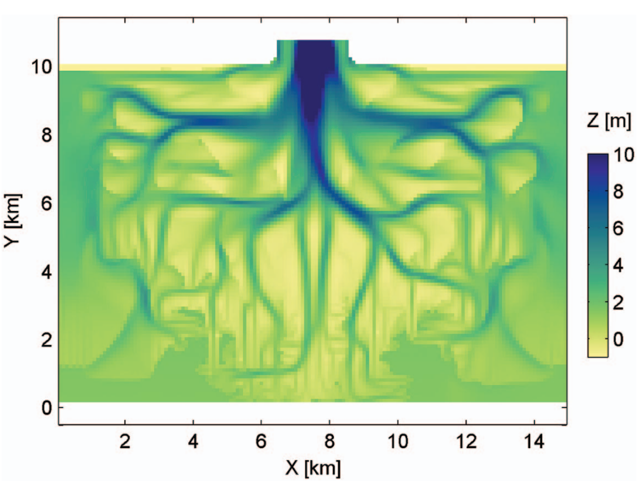

Fig. 8. (Color) Initial bed topography for the consolidation model, obtained from a 100-year morphodynamic simulation with 0.1 mm sand only and a 3 m symmetric tide at the inlet's mouth.

Table 3. Settings for the nonconsolidation simulations of schematized tidal inlet

ρ_{dry} (kg/m^3)	τ_{cr} (Pa)	M_E (s/m)
250	0.225	8.5×10^{-4}
800	0.225	4.8×10^{-6}

and $T_p = 6$ s, respectively, at the model's boundaries. The wind effects (flow and setup) were modeled with a wind velocity of 20 m/s.

The effect of consolidation was evaluated by comparison with two scenarios with sediment beds with constant properties. All the model scenarios (two without consolidation and one with consolidation) were forced with fine sediment entering the model domain through the inlet's mouth at a concentration of 0.1 g/L, a settling velocity of 0.25 mm/s, and the consolidation and erosion settings used in the first test case, see Consolidation Column. The DECON model results were compared with two scenarios without consolidation (the standard Delft3D): Scenario 1 had constant properties representing poorly consolidated sediments ($\rho_{dry} = 250$ kg/m^3), and Scenario 2 was set to represent highly consolidated sediments ($\rho_{dry} = 800$ kg/m^3); see Table 3. Note that the standard Delft3D uses the classical Partheniades erosion formulation (Ariathurai and Arulanandan 1978). Therefore, the erosion rate parameter in that model had to be modified to account for the fact that in the present model the erosion parameter was not normalized with the critical shear stress for erosion $[(\tau_b - \tau_e)/\tau_e \text{versus} (\tau_b - \tau_e)]$.

The results of the simulations are shown in Fig. 9 and presented in Table 4. Figs. 9(a, c, and e) show the model results after 25 years of a prolonged period of tide-only forcing, and Figs. 9(b, d, and f) show the model results after 25 years of composite forcing, that is, each year 10 months tide-only and then two months tide and waves. Without wave-induced resuspension, the basin was primarily depositional [Figs. 9(a, c, and e)]. Qualitatively, the deposition pattern by DECON [Fig. 9(a)] was comparable to the deposition pattern obtained from the traditional Delft3D simulations (without consolidation), using the constant low-density settings of $\rho_{dry} = 250$ kg/m^3; compare Figs. 9(a and c). In both simulations, the tidal channels remained basically clear of mud except near the head of the tidal basin, whereas throughout the model domain, the intertidal flats filled up with mud. However, the total amount of sediment in the tidal basin was only about half the amount computed for a constant ρ_{dry} (Table 4), indicating a lower effective trapping.

Increasing the dry-bed density in the traditional Delft3D simulation to $\rho_{dry} = 800$ kg/m^3 (thereby decreasing the erosion rate) yielded a different pattern, both qualitatively and quantitatively. Tidal channels then filled in and mud could no longer reach the head of the tidal basin [compare Fig. 9(e) with Fig. 9(a)], and the higher intertidal areas remained clear of mud. However, the total amount of fine sediment in the basin was about 50% greater than in the DECON simulation (Table 4). It can therefore be concluded that the high density settings failed to reproduce a realistic depositional pattern, whereas the low density settings and the consolidation model did reproduce realistic patterns, although the total amount of mud accumulation differed by a factor of 2.

Next, the effect of waves are discussed. The traditional Delft3D model at a high $\rho_{dry} = 800$ kg/m^3 predicted little effect of waves on the depositional patterns [compare Figs. 9(e and f)]; that is, the sediments deposited earlier were basically nonerodible, and they stayed on the intertidal area and within the channels. Although it was expected that there be a redistribution of earlier deposited sediments from the intertidal areas into the tidal channels during storms, as

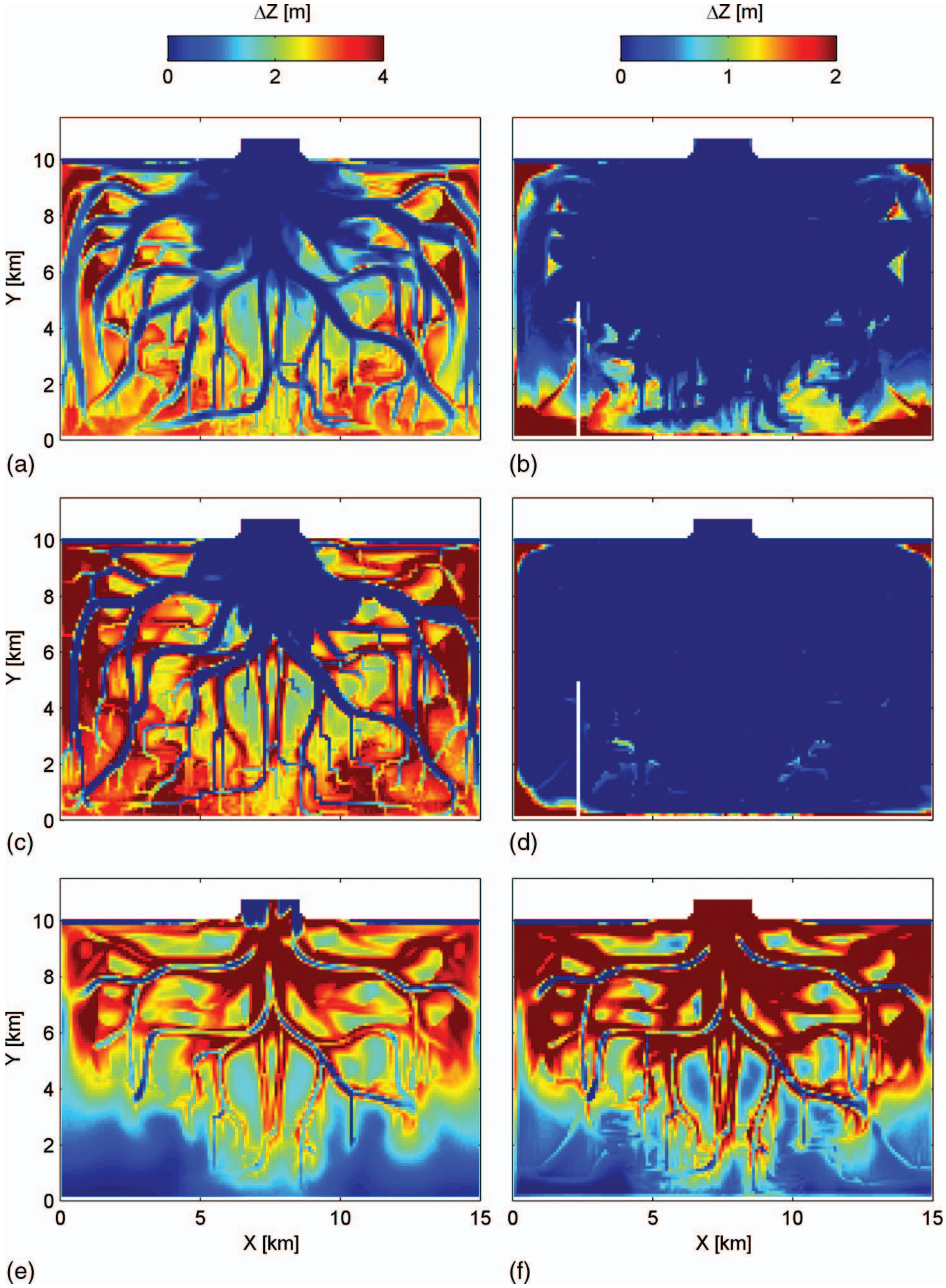

Fig. 9. (Color) Bed-level change after 25 years of mud infill; simulations (a, c, e) without waves; (b, d, f) with waves; (a and b) with the consolidation model; (c and d) with $\rho_{\rm dry} = 250\ {\rm kg/m^3}$; and (e and f) $\rho_{\rm dry} = 800\ {\rm kg/m^3}$. Note the different scales in simulations with and without waves. The white lines in (b) and (d) depict the locations of model output shown in Fig. 10.

Table 4. Computed sediment balance in tidal basin for the various simulations

Detail	Without waves (after 25 years)			With waves (after 25 years; each year 10 months tide only, 2 months tide + waves)		
Cons model	Yes	No	No	Yes	No	No
$\rho_{\rm dry}$ (kg/m^3)	By model	300	800	By model	300	800
Figure	Fig. 9(a)	Fig. 9(c)	Fig. 9(e)	Fig. 9(b)	Fig. 9(d)	Fig. 9(f)
Total mass (kg)	17.2×10^{10}	8.6×10^{10}	28.4×10^{10}	4.1×10^{10}	0.4×10^{10}	20.0×10^{10}

shown in Fig. 9(f), the accompanying export of fines from the basin was not predicted. In contrast, the waves did have a large impact in the Delft3D simulations with $\rho_{\rm dry} = 250\ {\rm kg/m^3}$ [Figs. 9(c and d)], predicting very low amounts of sediment accumulation in the computational domain (Table 4). The results of the DECON simulation lay between the results of these cases [Figs. 9(a and b)], predicting the erosion of all the sediments deposited during the summer on the tidal flats, but stable accumulations at the basin's head.

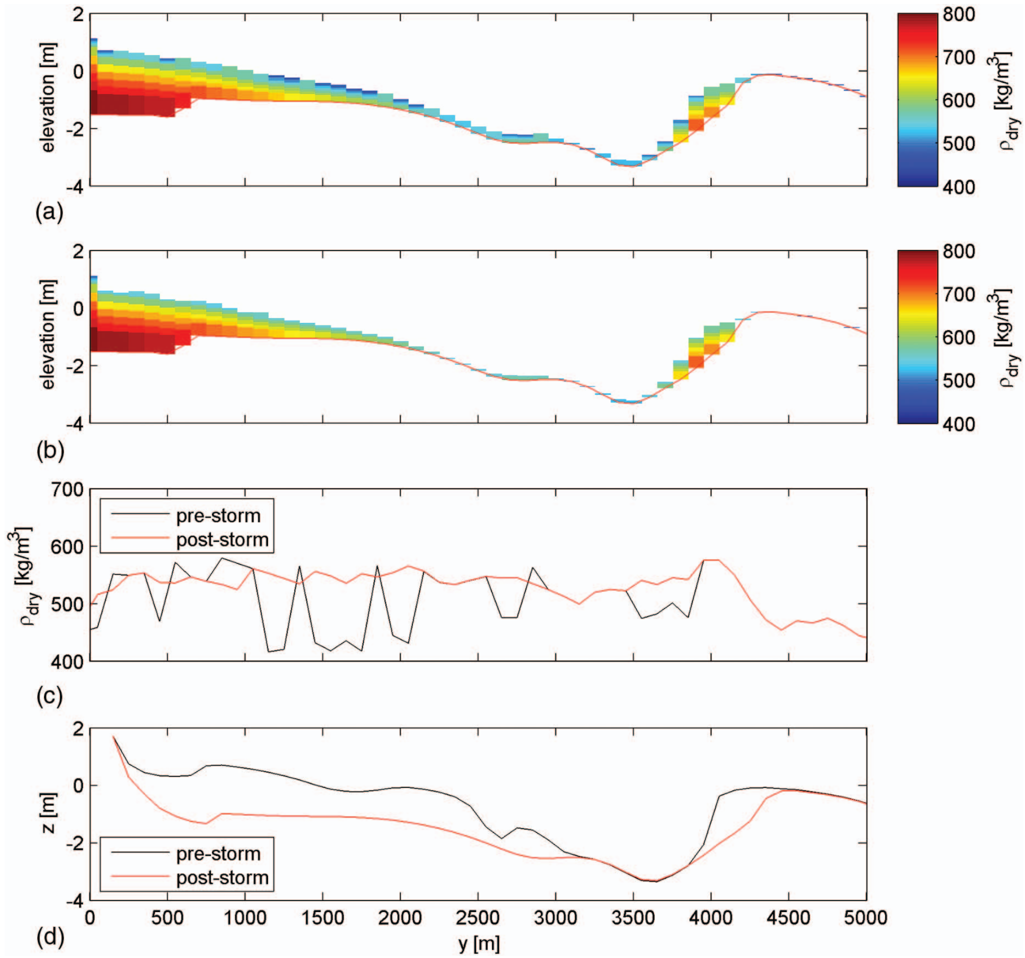

Fig. 10. (Color) Cross section of computed dry density: (a) before and (b) after a storm occurring in the 25th year of the model simulation; (c) the dry density of the near-surface layer for this simulation; and (d) the bed evolution of the model with low density and waves [corresponding to Fig. 9(d)] with the same pre- and post-storm conditions as (c). See Figs. 9(b and d) for the location of the transect.

The total amounts of mud in the model domain decreased by 75% (Table 4). The seasonal picture shown by Figs. 9(a and b) is in qualitative agreement with the observations of the Dutch Wadden Sea, where stable mud deposits at the head of the basins are found throughout the year (Van Ledden et al. 2004).

This strong impact of waves in the DECON simulations is further illustrated in Fig. 10, which shows dry density and bed level changes along the white lines in Fig. 9. Before the storm [Fig. 10(a)] the dry-bed density computed with DECON varied from >800 kg/m^3 at the head of the basin to ~400 kg/m^3 further seawards. Most sediment with a density below 500 kg/m^3 was eroded during the storm period [Fig. 10(b)] resulting in an increase in the surface dry density [Fig. 10(c)] and thus an enhanced resistance to erosion. However, the eroded layer was fairly thin, and the resulting bed-level changes were small [compare Figs. 10(a) with 10(b)]. In contrast, the simulations without consolidation and a low dry-bed density (thus, a large erosion rate parameter), showed unrealistically large storm-induced erosion rates as much as 2 m in two months' time.

From a more conceptual point of view, the left-hand pictures shown in Fig. 9 can be considered representative of summer conditions, when the wave forcing is small. In nature, the intertidal flats in the middle of tidal basins become progressively more muddy, in particular in the beginning of summer, when algae further stabilize these deposits (De Deckere et al. 2002). In wintertime, when waves become more prominent, these deposits are washed away and the intertidal areas in the middle of the basin become sandy. Moreover, the fines are washed out of the tidal basin to ambient waters. Our simulations showed that this seasonal behavior cannot be represented with one sediment setting, as in standard Delft3D. Only the use of a consolidation model, which accounts for the strengthening of the bed, allows the simulation of such seasonal behavior.

Discussion and Conclusions

In this paper, we proposed a fast consolidation model suitable for long-term morphodynamic simulations, on the basis of the assumption of dynamic equilibrium of the consolidating bed. We referred to the dynamic equilibrium consolidation (DECON) model. The DECON model was derived from existing consolidation theory, using Gibson's consolidation equation. The model's material parameters (hydraulic conductivity, consolidation coefficient, and strength) can therefore be derived from soil mechanical experiments in the laboratory.

Because of the equilibrium assumption, the effects of pore water flows are not explicitly accounted for, and water squeezed out of the bed during self-weight consolidation is not added to the water column, as that amount is generally negligible in natural systems (or rapidly compensated for through the open boundaries in a hydrodynamic model). The effects of pore water flow, induced by surface and/or tidal waves or by another cause, are also not accounted for, be it because no generally accepted approach is known. The effects of swelling during erosion is not included in updating the bathymetry, but swelling is implicitly included in the erosion formula.

The Gibson equation assumes isotropy. However, it is well known that in the thicker deposits of soft mud, drainage channels may be formed, which affect consolidation (e.g., Dankers 2006). Such drainage channels may also occur in shearing mud deposits. However, no theory/model based on first principles is known to account for such drainage channels, other than modifying the coefficients in the permeability model. As DECON was designed for low-concentration conditions, during which no thick layers of fluid mud are formed, drainage channels are likely not formed.

One could argue that the Gibson model combines the Kynch settling phase and Terzaghi's consolidation phase. During consolidation, the ratio between advection and diffusion (that is, the Kynch part and the Terzaghi part) changes, in the sense that the latter becomes more important over time. In DECON, this is not the case, and this ratio therefore depends on the soil at hand, that is, the soil's material parameters.

The effects of hindered settling in the DECON Delft3D software are accounted for in a hindered settling formula, which is solved in the SPM transport equation in the water column; the user may choose either the Richardson and Zaki formula (1954) or the formula proposed by Dankers and Winterwerp (2007). As a result, the first phase of the consolidation results in a concave-up density profile, whereas the latter phase yields an convex-up dry density profile. As DECON assumes equilibrium, the density profiles are convex-up, as shown in Figs. 2 and 4. Note that the Gibson equation can be derived fully from continuity, Darcy's law, and the concept of effective stresses. However, Gibson used the void ratio e and the material coordinates, whereas DECON uses the mass concentration of the solids (dry density) and Eulerian coordinates. DECON assumes self-similarity, yielding power laws for the material properties, that is, the hydraulic conductivity and effective stress [Eq. (2)]. This fractal approach also yields a power law for the undrained strength of the bed, which is used in our erosion model [Eq. (8)]. This Gibson approach is therefore very similar to, for instance, the model proposed by Diplas and Papanicolaou (1997), although using different independent parameters.

The DECON model is implemented into the generic bed model (GBM) of Deltares, which is coupled to Delft3D, but it can also be operated stand-alone and thus coupled to other models. The GBM is a multilayer bed model with a mixed Lagrangian-Eulerian vertical discretization for minimizing numerical diffusion and guaranteeing stable, positive solutions. In the Delft3D implementation, three computational time steps are eminent:

1. the time step for the hydrodynamic and sediment transport simulations, the latter including the water–bed exchange processes such as erosion and deposition Δt;
2. the consolidation time step T_c, which is a multiple of Δt, ruling the update of the mechanical properties of the consolidating bed (e.g., thickness, dry-density profile, sediment composition, and erodibility); and
3. the morphodynamic time step T_m, which governs the update of the bathymetry, modifying the hydrodynamics.

A proper understanding of these time scales and their evaluation during the setup of a model is a crucial step in obtaining sensible results with the model. The DECON model is coupled to the erosion formulae in Winterwerp et al. (2012), which contains soil mechanical parameters deployed within the consolidation model. This erosion model implicitly presumes swelling during erosion. Note that Sanford (2008) explicitly included an empirical swelling term in his consolidation model.

The DECON model is applicable for muddy systems. The mud may contain some sand, which is treated as a passive substance affecting only the consolidation parameters. DECON assumes quasi-equilibrium of the consolidating bed, which implies that DECON is applicable only when the sedimentation rates are not large. In fact, these sedimentation rates have to be considerably smaller than the consolidation rate, as in the case of low-concentrated environments. For high-concentrated environments, the full Gibson consolidation model should be considered (e.g., Zhou et al. 2016). From a simple order-of-magnitude estimation, we can assess the applicability of the model in more quantitative terms.

Let us assume that settling occurs mainly around slack water periods that are relatively short and that then all the sediment settles from the water column. The sedimentation rate thus equals the amount of sediment collected on the bed, divided by half the tidal period, that is, the time between two successive slack water deposits. The consolidation rate in the initial phase of consolidation is governed by the hydraulic conductivity of the deposit. This we may elaborate

$$\text{DECON applicable if: } F_s \ll F_c$$

$$F_s = \frac{c}{\rho_{\text{dry}}}\frac{h}{T/2} \quad \text{and} \quad F_c = K_k \phi_s^{-2/(3-n_f)}; \text{with } \phi_s = \rho_{\text{dry}}/\rho_s \tag{10}$$

where F_s and F_c = sedimentation and consolidation flux; c = SPM concentration in water column; ρ_{dry} and ρ_s = dry-bed and specific sediment density; h = water depth; K_k = hydraulic conductivity parameter; ϕ_s = solids volume concentration; and n_f = fractal dimension. As an example, let us assume a water depth of 5 m, and an SPM concentration of 0.1 g/L, whereas ρ_{dry} and ρ_s are 100 and 2,650 kg/m^3, respectively; $K_k = 1.59 \times 10^{-13}$ m/s; and $n_f = 2.69$ (as provided in Table 2). Substitution into Eq. (10) yields $F_s = 2.2 \times 10^{-7}$ m/s and $F_c = 2.4 \times 10^{-4}$ m/s; hence $F_s \ll F_c$, and for this example, one may apply quasi-equilibrium conditions.

Our aim was to develop a fast consolidation model for morphodynamic simulations. The simulations without waves for the schematized tidal inlet required a computational time about five times larger than in the case of a traditional nonconsolidation model (a 400% overhead). In the case that waves were included in the simulations, this overhead dropped to about 100%; that is, including the dynamic equilibrium consolidation required twice as much computational time. The tidal inlet model could not be run with the full Gibson equation, as the computational times would have become excessive. The DECON model can account for various mud and sand fractions in the water column. Within the bed, the mud and sand fractions are lumped, jointly determining the material properties for consolidation. Sand is treated as a passive substance, although affecting the conductivity and effective strength. All fractions are mixed homogeneously over a computational grid, and thus the effects of bed stratification can be resolved only at the resolution of the computational grid.

The DECON model has been evaluated qualitatively against schematized test cases, as no detailed long-term observations are available to the authors. The trends predicted by DECON are credible, showing model behavior that cannot be obtained with the traditional fine sediment transport models. However, we realize that the DECON approach will have to prove its value in large-scale applications in engineering studies.

Traditional numerical models simulating the transport and fate of the fine sediments in open water systems are calibrated by tuning the erosion and deposition fluxes from/onto the sediment bed. We do not discuss tuning sediment input/export over open boundaries, which is equally important. These fluxes are classically described by the Partheniades-Krone boundary conditions (Ariathurai and Arulanandan 1978), which contain four parameters (the critical shear stresses for erosion and deposition, an erosion parameter, and a settling velocity). In general, it is assumed that these parameters are constant in time and space and are fully empirical, obtained from model sensitivity runs or, at best, from some limited laboratory/field experiments.

At first sight, the DECON model seems in need of many more parameters. This is the inevitable price for introducing explicit descriptions for the soil mechanical response to hydrodynamic stresses. In the DECON approach, the critical shear stress for erosion and the erosion parameter are explicitly related to the soil mechanical properties of a consolidating bed. These parameters can be obtained from standard soil mechanical laboratory experiments. The consolidation and mechanical parameters (K_k, K_p, K_y, n_f, and c_u, where Γ_c follows from K_p, K_y, and n_f) follow from settling tests and vane tests. The Atterberg limits–related parameters (PI, A, and ξ_{cr}) follow from the activity plots. The empirical model parameters $D_{m,50}$, χ_{cr}, and β have been studied previously, and the recommended values are given. The ratio α_{cl} between the silt and clay fractions follows from grain-size analyses and is fairly constant for a particular open water system. We introduced a bioturbation parameter K but did not further elaborate or specify it; that remains for future work. The model needs the input of a settling velocity, as in traditional models. Two extra numerical parameters are required: T_c, the time scale for updating the mechanical bed properties, and m_{rel}, a parameter for smoothing the model response to changes in the hydrodynamic forcing. The parameters α_E and α_τ allow spatial variability in the model response, which would also be a logical expansion of traditional models but are set to unity as default values.

Appendix. Consolidation and Erosion

This appendix describes the equations for the sediment mass balance for the three layers (fluffy, active, and bed) used in the consolidation model. We presume that the burial of mud from the fluffy layer into the upper active layer (the first consolidating layer) is governed only by the permeability of the fluffy layer. In terms of the consolidation model, this implies the first is consolidation phase governed by the hydraulic conductivity defined by Merckelbach and Kranenburg (2004b)

$$\frac{\partial c_{m,f}}{\partial t} - \frac{1}{\rho_s}\frac{\partial}{\partial z}[\Delta_\rho k(c_{m,f})^2] = 0 \tag{11}$$

where $c_{m,f}$ = mass concentration of the mud fraction in the fluffy layer; Δ_ρ = relative density $\Delta_\rho = (\rho_s - \rho_w)/\rho_w$, and k = hydraulic conductivity. As the dry density of the fluffy layer will amount to about the gelling concentration, it is obvious to set $c_{m,f} \equiv c_{gel}$, which is a user-defined input parameter that follows from laboratory experiments and that is kept constant throughout the computational domain and with time. Integration over the (unknown) thickness δ_f of the fluffy layer yields the flux at the interface between the fluffy layer and the first active layer

$$\int_{\delta_{fl}} \frac{\partial c_m}{\partial t}\mathrm{d}z = \frac{\partial}{\partial t}\int_{\delta_{fl}} c_m \mathrm{d}z + c_m \frac{\partial \delta_{fl}}{\partial t} = \frac{\partial m_f}{\partial t} = -\frac{\Delta_\rho k c_m^2}{\rho_s} \tag{12}$$

as $c_{m,f} \equiv c_{gel} =$ constant. This implies that the mass balance of the fluffy layer is

$$\begin{aligned} &\frac{\mathrm{d}m_f^m}{\mathrm{d}t} = D_f^m - E_f^m - B_f^m \\ &D_f^m = e_d W_{s,b}^m C_b^m \\ &E_f^m = \xi^m M_{e,f}(\tau_b - \tau_{cr,f}) \quad M_{e,f} = \min\{m_f^m M_{f,1}, M_{f,0}\} \\ &B_f^m = \xi^m \min\{m_f^m P_{f,1}, P_{f,0}\};\ \text{where} \quad P_{f,0} = \Delta_\rho k c_m^2/\rho_s \end{aligned} \tag{13}$$

$$\frac{\mathrm{d}m_f^s}{\mathrm{d}t} = D_f^s - B_f^s = 0 \quad \text{and} \quad m_f^s = 0 \qquad \text{no sand in fluffy layer} \tag{14}$$

In these equations, we have defined D = deposition rate; E = erosion rate; and B = burial rate. Remember that superscripts m and s refer to the mud and sand class, respectively, whereas subscripts m and s refer to the total (or bulk) mud and sand content. For the first-order consolidation term $P_{f,1}$ we take the same function as for the erosion rate, accounting for a reduction in mass in the fluffy layer, as subsequently discussed. The role of the efficiency for deposition e_d is discussed at the end of this appendix.

The mass balance of the first active sublayer (first consolidating layer) is

$$\begin{aligned} &\frac{\partial m_{AL1}^m}{\partial t} = B_f^m - E_{AL1}^m + F_{AL1,2}^m \\ &\xi_{AL1}^m = m_{AL1}^m/\mathrm{Mass}_{AL1}; \quad c_{AL1}^m = m_{AL1}^m/\delta_{AL1} \\ &E_{AL1}^m = \xi_{AL1}^s M_{e,AL1}(\tau_b - \tau_{cr,f})R_{\mathrm{rel}} \quad \text{for } \tau_b > \tau_{cr,f} \\ &F_{AL1,2}^m = -K_{AL1,2}\frac{\partial(c_{AL1,2}^m)}{\partial z} \end{aligned} \tag{15}$$

$$\begin{aligned} &\frac{\partial m_{AL1}^s}{\partial t} = D_{AL1}^s - E_{AL1}^s + F_{AL1,2}^s \\ &\xi_{AL1}^s = m_{AL1}^s/\mathrm{Mass}_{AL1}; \quad c_{AL1}^s = m_{AL1}^s/\delta_{AL1} \\ &D_{AB1}^s = W_b^s C_b^s \\ &E_{AL1}^s = \xi_{AL1}^s M_{e,AL1}(\tau_b - \tau_{cr,f})R_{\mathrm{rel}} \quad \text{for } \tau_b > \tau_{cr,f} \\ &F_{AL1,2}^s = -K_{AL1,2}\frac{\partial(C_{AL1,2}^s)}{\partial z} \end{aligned} \tag{16}$$

$$\frac{\mathrm{d}(\mathrm{Mass}_{AL1})}{\mathrm{d}t} = \sum_m^M \frac{\mathrm{d}m_{AL1}^m}{\mathrm{d}t} + \sum_s^S \frac{\mathrm{d}m_{AL1}^s}{\mathrm{d}t} \quad \text{and}$$
$$\frac{\mathrm{d}\delta_{AB1}}{\mathrm{d}t} = \sum_m^M \frac{\mathrm{d}m_{AL1}^m}{c_{dry}^m \mathrm{d}t} + \sum_s^S \frac{\mathrm{d}m_{AL1}^s}{c_{dry}^s \mathrm{d}t} \tag{17}$$

where F = diffusion rate between the layers, for example, due to bioturbation. K is then a bioturbation-induced diffusion coefficient. We have introduced a relaxation coefficient in the erosion formula to prevent a too-stiff response of the erosion properties after updating the bed strength (dry density): $R_{rel} = (1 - \exp\{m_{\mathrm{rel}}\Delta t/T_c\})$. Here, Δt = computational time step, and m_{rel} = user-defined relaxation coefficient for erosion. For example, for $m_{rel} = 0.3T_c/\Delta t$, one would attain 95% of the equilibrium erosion rate in 10 time steps.

The mutual exchange of mass between the various active sublayers underneath, between the various Eulerian bed layers underneath, and between the last active sublayer (e.g., the last consolidating layer) and the upper Eulerian bed layer takes place through bioturbation only.

In the upper layers, a mixed zero-/first-order erosion model is used, accounting for a possible depletion of those layers from

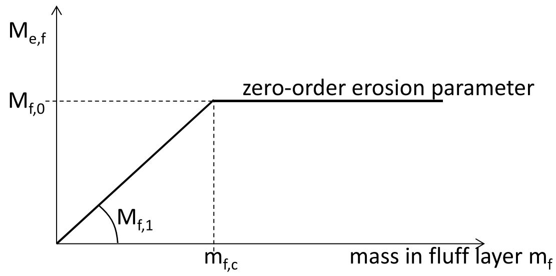

Fig. 11. Zero- and first-order erosion rates.

sediments. The behavior of the erosion parameter M_{ef} is shown in Fig. 11.

The zero-order erosion rate follows from Winterwerp et al. (2012)

$$E = \alpha_E \frac{\Gamma_c \rho_{m,dry}^2}{10\rho_s c_u D_{m,50}}(\tau_b - \tau_{cr})\left(1 - \exp\left\{\frac{m_{rel}\Delta t}{T_c}\right\}\right) \equiv \alpha_E M_E(\tau_b - \tau_{cr}) R_{rel} \quad (18)$$

where the erosion parameter M_E has the dimension $\mathrm{kg/m^2\,s\,Pa} \equiv \mathrm{s/m}$. Further, we introduce α_E, a user-defined calibration parameters, which may vary horizontally (x, y) over the computational domain (for example, different in channel and on tidal flat), and may vary per layer (z).

The undrained strength c_u is approximated by the yield strength (e.g. Winterwerp and Van Kesteren 2004), again assuming self-similar behavior (Kranenburg 1994)

$$c_u \approx \tau_y = K_y(\phi_m/(1-\phi_s))^{2/(3-n_f)} \quad (19)$$

where the coefficient for yield strength K_y (Pa) follows from the laboratory analyses (user input). The critical shear strength for erosion is related to the plasticity index PI of the sediment mixture

$$\tau_{cr} = \alpha_\tau \gamma_{cr} \mathrm{PI}^\beta \quad \text{with } \beta = 0.2 \text{ and } \gamma_{cr} = 0.7\,\mathrm{Pa}(0.35 < \gamma_{cr} < 1.4\,\mathrm{Pa})$$
$$\mathrm{PI} = A(X^{cl} - X_{cr}^{cl}) \quad \text{with PI in } [\%]$$
$$X^{cl} = \alpha_{cl} X^{mud} \text{ assuming a constant clay silt ratio,}$$
$$\alpha_{cl} \text{ user-defined input} \quad (20)$$

where $\alpha_\tau(x, y, z)$ is a user-defined calibration parameter, which may vary horizontally (x, y) over the computational domain (for example, different in channel and on tidal flat) and may vary per layer (z). The following parameters are user input (constant for the entire computational domain): K_k, K_p, K_y, n_f, D_{50}, ρ_s, A, ζ_{cr}^{cl}, and α_{cl}; all can be obtained from soil mechanical analyses of soil samples from the sea/river bed to be studied. The parameters β and γ_{cr} in the erosion model are also user input (with default values given).

In the deposition rate for muddy sediments, a deposition efficiency e_d is

$$D = e_d W_s c_b \quad (21)$$

This deposition rate models two aspects that are not properly accounted for in a sediment transport model (see also Van Kessel et al. 2012):

1. Horizontal grid resolution—deposition on a sandy substrate. In the case of a sand-mud mixture, where the sea/river bed consists of a sandy substrate, bed forms are likely. That would imply that the deposition of fines is spatially restricted to the troughs of the bed forms, that is, a certain fraction of the area covered by a computational grid.
2. Vertical grid resolution—hindered settling. It is noteworthy that even at fairly small depth-mean SPM concentrations of a few 100 mg/L, near-bed SPM values can become large. The near-bed sediment settling velocity is thus affected by hindered settling, substantially reducing the actual deposition flux. In engineering models, the vertical resolution of the computational grid is rarely fine enough to resolve the associated sediment concentration gradients near the bed. In such cases, properly accounting for these hindered settling effects may require an efficiency deposition coefficient of about 10%.

It is noteworthy that this deposition efficiency differs fundamentally from the critical shear stress for deposition, often used in the Krone deposition formula (Ariathurai and Arulanandan 1978), which relates deposition to the bed shear stress, accounting for a lack in resolving vertical mixing. By default, and in the applications presented in this paper, the deposition efficiency is set to 1, as in standard deposition models.

Acknowledgments

The Generic Bed Model was developed under the supervision of Thijs van Kessel and Bert Jagers, financed through the Ecoshape Building with Nature project NTW 1.3 Mud Dynamics. The new consolidation model was conceptualized and derived by Han Winterwerp, implemented in Delft3D by Zeng Zhou, and tested and debugged by Giulia Battista. Bas van Maren, Mick van der Wegen, and Bert Jagers assisted in the Delft3D applications. Work on the consolidation model was financed from Deltares's strategic research funds (Programme Coastal and Offshore Engineering). Zeng Zhou is supported by the Jiangsu Provincial Natural Science Foundation (Grant BK20160862), the National Natural Science Foundation of China (Grants 41606104 and 51620105005), and the Fundamental Research Funds for the Central Universities (Grant 2016B00714).

References

Ariathurai, C. R., and K. Arulanandan. 1978. "Erosion rates of cohesive soils." *J. Hydraul. Div.* 104 (2): 279–282.

Bartholomeeusen, G., et al. 2002. "SIDERE: Numerical prediction of large strain consolidation." *Géotechnique* 52 (9): 639–648. https://doi.org/10.1680/geot.2002.52.9.639.

Been, K., and C. G. Sills. 1981. "Self-weight consolidation of soft soils: An experimental and theoretical study." *Géotechnique* 31 (4): 519–535. https://doi.org/10.1680/geot.1981.31.4.519.

Blom, A. 2003. "A vertical sorting model for rivers with non-uniform sediment and dunes." Ph.D. thesis, Delft Univ. of Technology.

Dankers, P. J. T. 2006. "On the hindered settling of suspensions of mud and mud-sand mixtures." Ph.D. thesis, Delft Univ. of Technology.

Dankers, P. J. T., and J. C. Winterwerp. 2007. "Hindered settling of mud flocs: Theory and validation." *Cont. Shelf Res.* 27 (14): 1893–1907. https://doi.org/10.1016/j.csr.2007.03.005.

De Deckere, E. M. G. T., B. A. Kornman, N. Staats, G. R. Termaat, B. De Winder, L. J. Stal, and W. G. M. Heip. 2002. "The seasonal dynamics of benthic (micro)organisms and extracellular carbohydrates in an intertidal mudflat and their effect on the concentration of suspended sediment." Vol. 5 of *Fine sediment dynamics in the marine environment*, edited by J. C. Winterwerp and C. Kranenburg, 429–440. Amsterdam, Netherlands: Elsevier.

Diplas, P., and A. N. Papanicolaou. 1997. "Batch analysis of slurries in zone settling regime." *J. Environ. Eng.* 123 (7): 659–667. https://doi.org/10.1061/(ASCE)0733-9372(1997)123:7(659).

Gibson, R. E., G. L. England, and M. J. L. Hussey. 1967. "The theory of one-dimensional consolidation of saturated clays." *Géotechnique* 17 (3): 261–273. https://doi.org/10.1680/geot.1967.17.3.261.

Kranenburg, C. 1994. "On the fractal structure of cohesive sediment aggregates." *Estuarine Coastal Shelf Sci.* 39 (5): 451–460. https://doi.org/10.1006/ecss.1994.1075.

Mathew, R., and J. C. Winterwerp. 2017. "Surficial sediment erodibility from time-series measurements of suspended sediment concentrations: Development and validation." *Ocean Dyn.* 67 (6): 691–712. https://doi.org/10.1007/s10236-017-1055-2.

Merckelbach, L., and C. Kranenburg. 2004a. "Determining effective stress and permeability equations for soft mud from simple laboratory experiments." *Géotechnique* 54 (9): 581–591. https://doi.org/10.1680/geot.2004.54.9.581.

Merckelbach, L., and C. Kranenburg. 2004b. "Equations for effective stress and permeability of soft mud-sand mixtures." *Géotechnique* 54 (4): 235–243. https://doi.org/10.1680/geot.2004.54.4.235.

Mitchell, J. K. 1976. *Fundamentals of soil behaviour*. New York: Wiley.

Postma, H. 1961. "Transport and accumulation of suspended matter in the Dutch Wadden Sea." *Neth. J. Sea Res.* 1 (1–2): 148–190. https://doi.org/10.1016/0077-7579(61)90004-7.

Richardson, J. F., and W. N. Zaki. 1954. "Sedimentation and fluidization: Part I." *Trans. Inst. Chem. Eng.* 32: 35–53.

Roelvink, J. A. 2006. "Coastal morphodynamic evolution techniques." *Coastal Eng.* 53 (2–3): 277–287. https://doi.org/10.1016/j.coastaleng.2005.10.015.

Sanford, L. 2008. "Modeling a dynamically varying mixed sediment bed with erosion, deposition, bioturbation, consolidation, and armoring." *Comput. Geosci.* 34 (10): 1263–1283. https://doi.org/10.1016/j.cageo.2008.02.011.

Schiffman, R. L., V. Pane, and V. Sunara. 1985. "Sedimentation and consolidation." In *Flocculation, sedimentation and consolidation*, edited by B. M. Moudgil and P. Somasundaram, 57–124. Gainesville, FL: Univ. of Florida.

Sloff, C. J., H. R. A. Jagers, E. Kobayashi, and Y. Kitamura. 2006. "Enhanced flushing of sediment deposits in the backwater reach of reservoirs." In *Proc., River, Coastal and Estuarine Morphodynamics: RCEM 2005*, 483–491. London: Taylor and Francis Group.

Terzaghi, K. 1943. *Theoretical soil mechanics*. New York: Wiley.

Toorman, E. 1996. "Sedimentation and self-weight consolidation: General unifying theory." *Géotechnique* 46 (1): 103–113. https://doi.org/10.1680/geot.1996.46.1.103.

Townsend, F. C., and M. C. McVay. 1990. "SOA: Large strain consolidation predictions." *J. Geotech. Eng.* 116 (2): 222–243. https://doi.org/10.1061/(ASCE)0733-9410(1990)116:2(222).

Van Kessel, T., A. Spruyt-de Boer, J. Van der Werff, L. Sittoni, B. Van Prooijen, and J. C. Winterwerp. 2012. *Bed module for sand-mud mixtures*. Technical Rep. No. 1200327. Delft, Netherlands: Deltares.

Van Kessel, T., J. C. Winterwerp, B. Van Prooijen, M. Van Ledden, and W. Borst. 2011. "Modelling the seasonal dynamics of SPM with a simple algorithm for the buffering of fines in a sandy seabed." *Cont. Shelf Res.* 31 (10): S124–S134. https://doi.org/10.1016/j.csr.2010.04.008.

Van Ledden, M., Z. B. Wang, J. C. Winterwerp, and H. De Vriend. 2004. "Sand-mud morphodynamics in a short tidal basin." *Ocean Dyn.* 54 (3–4): 385–391. https://doi.org/10.1007/s10236-003-0050.

van Rijn, L. C. 2007a. "A unified view of sediment transport by currents and waves. Part 1: Initiation of motion, bed roughness and bed load transport." *J. Hydraul. Eng.* 133 (6): 649–667. https://doi.org/10.1061/(ASCE)0733-9429(2007)133:6(649).

van Rijn, L. C. 2007b. "A unified view of sediment transport by currents and waves. Part II: Suspended transport." *J. Hydraul. Eng.* 133 (6): 668–689. https://doi.org/10.1061/(ASCE)0733-9429(2007)133:6(668).

van Straaten, L. M. J. U., and P. H. Kuenen. 1957. "Accumulation of fine grained sediments in the Dutch Wadden Sea." *Geologie en Mijnbouw* 19: 329–354.

Winterwerp, J. C. 1999. "On the dynamics of high concentrated mud suspensions." Ph.D. thesis, Delft Univ. of Technology.

Winterwerp, J. C., and W. G. M. Van Kesteren. 2004. "Introduction to the physics of cohesive sediment dynamics in the marine environment." Vol. 56 of *Developments in sedimentology*, Amsterdam, Netherlands: Elsevier.

Winterwerp, J. C., W. G. M. Van Kesteren, B. Van Prooijen, and W. Jacobs. 2012. "A conceptual framework for shear-flow induced erosion of cohesive sediment beds." *J. Geophys. Res.* 117 (C10): C10020. https://doi.org/10/1029/2012JC008072.

Zhou, Z., M. Van der Wegen, B. Jagers, and G. Coco. 2016. "Modelling the role of self-weight consolidation on the morphodynamics of accretional mudflats." *Environ. Modell. Software* 76: 167–181. https://doi.org/10.1016/j.envsoft.2015.11.002.

J. Hydraul. Eng., 2018, 144(8): 04018055